EFFECT OF SOIL PARTICLE SIZE ON THE ELECTROCHEMICAL CORROSION BEHAVIOR OF PIPELINE STEEL IN SALINE SOLUTION

B. HE [1, 3], *P. J. HAN* [1, 2], *C. H. LU* [3], *X. H. BAI* [1]

[1] *College of Architecture and Civil Engineering, Taiyuan University of Technology, P. R. China;*

[2] *College of Materials Science and Engineering, Taiyuan University of Technology, P. R. China;*

[3] *Department of Civil Engineering, Monash University, Clayton, Australia*

In this study, by using a standard quartz replace of sandy soil particles, the effect of soil particle size (0.1…0.25 mm, 0.6…1.0 mm) on the electrochemical corrosion behavior of X70 pipeline steel in sandy soil corrosive environment simulated by 3.5 wt.% sodium chloride (NaCl) was investigated through polarization curve and electrochemical impedance spectroscopy (EIS) technology. The results indicated that the polarization resistance of X70 steel decreased with a decreasing particle size. For all polarization curves the right shift of cathodic branch with a decreasing particle size is observed. The corrosion of X70 steel is controlled by the cathode process diffusion and oxygen reduction at the metal-environment interface, the intensity of which increases with the decreasing particle size.

Keywords: *sandy soil corrosion, particle size, X70 pipeline steel, gas/liquid/solid three-phase boundary (TPB) zone, polarization curve.*

With the increasing service life of West-East gas pipeline project in China, the problem of underground pipeline due to soil corrosion becomes increasingly serious [1]. The line of No.1 West-East gas pipeline project of underground pipeline engineering mainly uses X70 steel, and about 4000km long pipeline is buried in the desert of saline soil area in Northwest China [2]. The soil corrosion process of the underground metal structure is influenced by many factors, such as water content, chemical composition, environmental pH value, the electrical resistivity, soil type, salinity, noise, porosity and other factors. The effect of these factors has been investigated by many researches [3–7]. However, the effect of soil particle size on the electrochemical corrosion behavior of the underground metal structure is not fully understood, as corrosion mechanism in soil environment has not been fully investigated.

Although the influence of TPB zone on the corrosion behavior of metals has been investigated in solution and atmospheric environment, not enough research has been done on the effect of the particle size on corrosion behavior of metals exposed to soil. Authors of study [8] reported the effect of particle size on electrochemical corrosion behavior of steel in a sandy soil corrosion system for the first time. The results of Wang and other researchers [8–12] show that the corrosion behavior of metals is influenced by the dispersion degree of electrolytic liquid droplets on the metal surface which is determined by the soil particle dispersion effect, which also causes the electrolyte discontinuous distribution on the metal surface [10]. Sandy soil is a highly dispersed porous corrosion system that results in atmospheric oxygen movement along the pore to the electrode surface, which is a typical gas/liquid/solid multiphase corrosion system. Authors of [9–12] also introduced the TPB zone concept, which is a gas/liquid/solid three-phase boundary to the liquid phase area from 0 to 100 mm thickness of liquid film within the liquid phase reaction area to explain the influence of the par-

Corresponding author: X. H. BAI, e-mail: bxhong@tyut.edu.cn

ticle size on the corrosion behavior of metal. Comparing with the reaction area of liquid phase in general, the TPB zone is a high-speed cathodic reaction zone, in which the diffusion rate of oxygen is much higher than that in the bulk solution [13] and the metals suffer more severe corrosion with the increase of TPB length per unit area. Thus, the TPB zone plays a key role in understanding how particle size influences the corrosion of the cathode process of the buried steel. In the highly dispersed liquid corrosion system such as gas/liquid/solid multiphase sandy soil corrosion system, specifically, the TPB zone may even become the dominant factor of corrosion process and the cathodic oxygen reduction reaction will control the corrosion process, which also confirms that the liquid dispersion degree accelerates the metal corrosion process [14, 15].

The main methods of studying the corrosion behavior of the underground metal structure in the soil corrosion system include a weight-loss method, polarization curve, electrochemical impedance spectroscopy (EIS), the application of scanning electron microscopy (SEM), energy spectrum analysis and X-ray diffraction (XRD) analysis of the microstructure and corrosion product layer on the metal surface. In order to investigate the corrosion behavior of metals in soil, especially in sandy soil which is a high impedance multiphase corrosion system, a suitable method is chosen. However, the soil is defined as an electrolyte and this can be investigated by means of the electrochemical theory. Furthermore, the EIS technology is a very effective tool for studying the metal/soil corrosion system [16, 17] with small perturbation of the measured system and insensitive to the medium of the IR resistivity drop. The influence of the soil particle size on cathode reaction process of metal corrosion is significant, however, the polarization curve of cathode branch can reflect the cathodic process effectively, thus it is also an effective method to study the corrosion rate of metal [18, 19].

So, in this investigation, the polarization curves technique, electrochemical impedance spectroscopy (EIS) combined with scanning electron microscopy (SEM) and X-ray diffraction techniques were used. It is expected that a better understanding will be obtained on the effect of the particle size on the electrochemical corrosion behavior of X70 pipeline steel in 3.5 wt.% NaCl simulating sandy soil corrosive environment.

Materials and experimental procedure. ***Materials*****.** As a test soil the commercially available 99.2% quartz sand (China ISO) was used. The particle sizes of soil samples are: 0.1…0.25 mm (1# sands); 0.6…1.0 mm (2# sands). The quartz sand was ultrasonically cleaned in deionized water and dried naturally for 24 h before experiment. The simulated soil corrosive environment was 3.5 wt.% NaCl sandy soil corrosive system, prepared by the analytical grade chemical reagent of pure sodium chloride and deionized water, with the water content of 18%. Each soil sample (450 g) was manually compacted inside the experimental installation using a Proctor Compactor, as shown in Fig. 1, controlling the dry density of 1.65 g/cm^3, which means that the porosity of sandy soil corrosion system equals 0.38. Furthermore, the top of the device was sealed with the waterproof breathable layer in order to ensure constant water content throughout the experiment process.

The X70 pipeline steel with the main chemical composition (0.0645wt.% C; 0.201 wt.% Si; 1.906wt.% Mn; 0.0119wt.% P; < 0.0005wt.% S; 0.021wt.% Cr; 0.021wt.% Ni; 0.234wt.% Mo; 0.012wt.% Cu; 0.013wt.% Co; 0.011wt.% V; balance Fe) was used for this investigation. The specimens consisted of 15×15×2 mm (width×length× ×thickness) plates and the working surface area was polished using a series of silicon carbide emery papers of grades 400; 600; 800; 1000; 1200 to 1500 grit, respectively. The samples were enlaced with copper conductor around the borders, and then covered with epoxy resin except of the working area of 10×10 mm. Finally specimens were cleaned with ethanol, followed by rinsing with deionized water, degreased with alcohol, and then dried naturally before buried test.

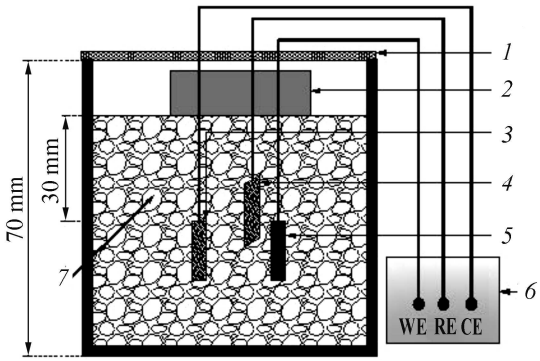

Fig. 1. The schematic diagram of the electrochemical system designed for the study of the behavior of X70 pipeline steel in sandy soil corrosive environment: *1* – waterproof breathable layer; *2* – fixed board; *3* – counter electrode (platinum); *4* – reference electrode (SCE); *5* – X70 pipeline steel; *6* – electrochemical workstation (CS350); *7* – sandy soil.

Electrochemical measurement. All the electrochemical experiments were carried out by electrochemical workstation (CS350, manufactured by WUHAN CORRTEST INSTRUMENTS CO., China) at room temperature of 20±1°C and moisture of 45±2%. The conventional three electrodes was used: a platinum counter electrode, a saturated calomel electrode (SCE) as a reference electrode, the working electrode was the X70 steel buried in sandy soil as described above. All potentials were reported with respect to SCE.

The potentiodynamic polarization curves were recorded with a constant scanning rate of 0.167 mV/s, and the open-circuit potential was stable for 30 min before recording the polarization curves. The cathodic branch was always determined first, then the open circuit potential (OCP) was re-established followed by the anodic branch determination. The samples were polarized from –200 mV to 200 mV versus OCP. The experiments were performed for 7, 60 and 90 days, respectively, and the results were analyzed using the Tafel extrapolation method [19] and the fit program CView2 software.

Electrochemical impedance spectroscopy (EIS) measurements were conducted at the open circuit potential sine signal of 10 mV and in the 10^5 and 10^{-2} Hz frequency range. In order to reach stable conditions, 30 min were set before test. The results were analyzed using the fit program ZSimpWin software.

Surface characterization. In order to understand the corrosion process of X70 pipeline steel buried in the sandy soil corrosive environment, the surface morphologies of the buried samples were observed by scanning electron microscope (SEM), equipped with an energy dispersive X-ray spectroscopy (EDS) system (Hitachi High-Technologies TM3000) for elemental analysis, operating at 15 kV. Corrosion products of the specimens were removed with dilute hydrochloric acid solution for 10 min at 20°C. Furthermore, the corrosion products of X70 steel surface were removed and characterized by XRD after the electrochemical corrosion tests.

Results and discussion. ***Linear polarization resistance test variation with buried time.*** The linear polarization curves for X70 steel for different buried time were measured so that the corrosion rate of X70 steel could be monitored in the 3.5 wt.% NaCl soil corrosive environment with varying particle size. Fig. 2 displays the change of polarization resistance (R_p) of X70 steel obtained from the linear polarization curves as a function of buried time. It can be seen that the R_p values of X70 steel with different particle sizes both decrease linearly with the increase of buried time, and the R^2 is the goodness of fit. Moreover, the results of paper [20] showed that the polarization resistance is inverse proportional to the corrosion current density, which is inversely proportional to the corrosion rate of metal. Thus, it means that the corrosion rate of X70 steel increases with the buried time increasing. But, with the same buried time, the R_p values of X70 steel in 1# system are less than that in 2# sandy corrosion system, indicating that the corrosion rate of X70 steel increased with decreasing sandy soil particle size. This is because of the particle size decrease with increasing dispersion degree

of the electrolytic liquid droplets on the surface of the metal as well as increasing TPB length per unit area, and the significant effect acceleration of the cathode process of X70 steel which is controlled by the process of cathodic oxygen reduction [8, 13, 14]. Therefore, the corrosion rate of X70 steel is higher in the smaller particle size sandy soil corrosion system.

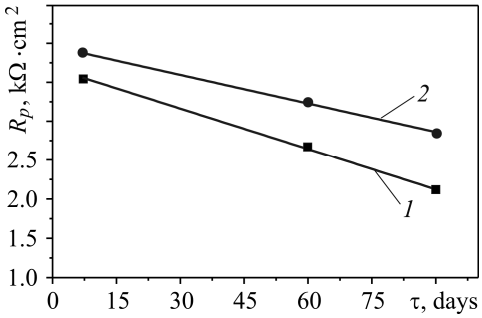

Fig. 2. The variation of R_p as a function of buried time with different particle sizes: *1* – 1# sands, R^2 = 0.991; *2* – 2# sands, R^2 = 0.996.

Potentiodynamic polarization curve measurements. Potentiodynamic polarization curve of X70 steel in 3.5 wt.% NaCl sandy soil corrosive environment with different particle size after buried 7, 60 and 90 days are recorded, as shown in Fig. 3. The obtained electrochemical corrosion kinetics parameters obtained using CView2 software, together with Tafel extrapolation method versus buried times are presented in Table 1. Obviously, for all polarization curves, they have the similar shapes indicating the same corrosion processes in them.

The Tafel slope (B_a) of anode branch is related to the dissolution of X70 steel electrode while the cathodic Tafel slope (B_c) corresponds to the oxygen reduction process of X70 steel corrosion. The anodic polarization curves are almost the same, because the Tafel slope (B_a) of anode branch is related to the dissolution of X70 steel electrode and increase with the buried time increasing. The increasing values of B_a with growing buried time is mainly a result of the increasing corrosion rate of X70 pipeline steel, which means that the dissolution rate for X70 steel increase with the buried time growth.

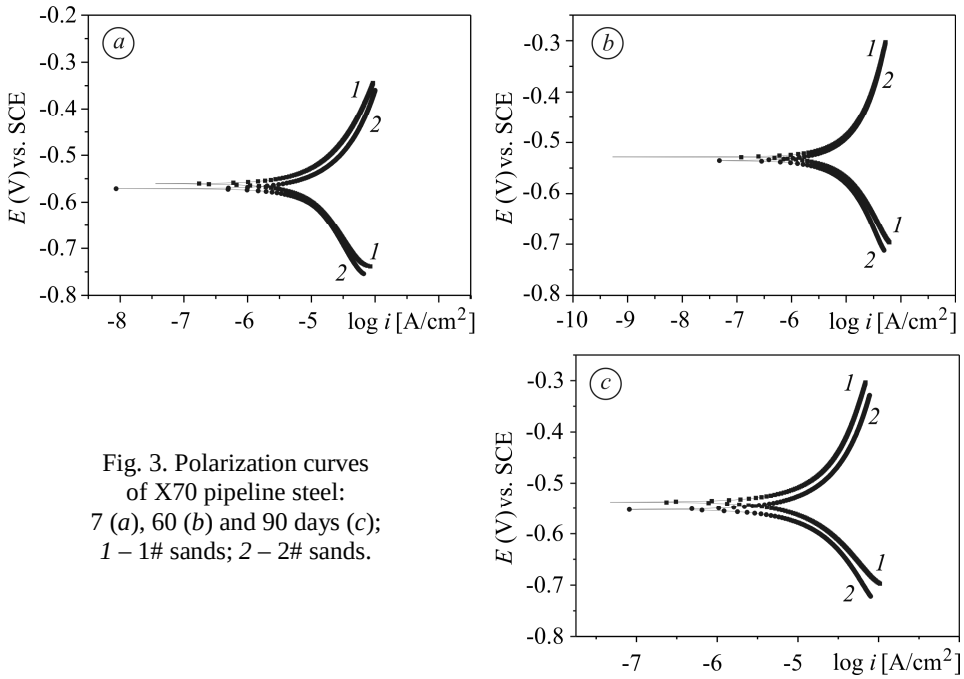

Fig. 3. Polarization curves of X70 pipeline steel: 7 (*a*), 60 (*b*) and 90 days (*c*); *1* – 1# sands; *2* – 2# sands.

The cathodic Tafel slope (B_c) corresponds to the oxygen reduction process of X70 steel corrosion. But for the cathode branch of polarization curve, the right shift of the cathodic branch with decreasing particle size, suggests that the cathode oxygen reduc-

tion process is accelerated and the metal corrosion is controlled by the cathodic oxygen reduction process. These results may be due to the proportion of TPB zone per unit area as well as the total cathodic current which increases with decreasing particle size. Compared to the corrosion potential (E_{corr}) when buried in 1# sandy corrosion system, the corrosion potential became less negative (from –561 to –572 VSCE after 7 days, from –528 to –536 VSCE after 60 days, and from –537 to –572 VSCE after 90 days,) in 2# sandy corrosion system. It is interesting to note that the corrosion potential is influenced by two processes: the cathodic and anodic [21]. In general, there are two reasons for a negative shift in corrosion potential; both the anodic and cathodic processes on the metal surface are promoted [22]. In Table 1 it can be also observed that with increase of the particle size from 0.1…0.25 to 0.6…1.0 mm, i_{corr} decreases from 8.797 to 8.589 μA/cm^2 after 7 days, from 6.789 to 6.019 μA/cm^2 after 60 days and from 10.112 to 10.050 μA/cm^2 after 90 days. Thus, the average current density supplied by the cathodic process is higher. The corrosion rate is closely related to the values of corrosion current density, and the corrosion rate for X70 steel increases with decreasing sandy soil particle size.

Table 1. Potentiodynamic polarization fitted data of X70 pipeline steel

Buried time	Sand numbers	E_{corr}, V	i_{corr}, μA/cm^2	B_a, mV/dec	B_c, mV/dec
7 days	1#	–561	8.797	287	–195
	2#	–572	8.589	302	–216
60 days	1#	–528	6.789	468	–194
	2#	–536	6.091	473	–233
90 days	1#	–537	10.112	529	–173
	2#	–572	10.050	506	–231

Electrochemical impedance spectroscopy measurements. The Nyquist (*a*, *c*, *e*) and Bode plots (*b*, *d*, *f*) of X70 steel corrosion in 3.5 wt.% NaCl sandy soil corrosive environment with buried time 7, 60, and 90 days, respectively, are shown in Fig. 4. All the Nyquist plots compose a capacitive loop at high frequency, capacitive arc at intermediate frequency and Warburg diffusive impedance in the low frequency range. It is also observed that there is a similarity among all Nyquist plots, i. e., a depressed semicircle with the center under the real axis, such behavior characteristics for soil corrosion system are attributed to the low electrical conductivity and higher impedance of soil for "dispersion effect" [23]. In the soil corrosion system, the generation of "dispersion effect" may be due to the adhesion of the combination of corrosion products with soil particles to the surface of metal electrode, which changes the condition of the electrode surface.

The high frequency capacitive loop corresponds to the characteristics of corrosion product film of the X70 steel which means the electron transfer of electrode surface is impeded, and it is associated with the condition of the electrode surface [24]. Furthermore, the size of high-frequency semicircle decreases with decreasing the particle size is ranging from 0.1…0.25 to 0.6…1.0 mm with buried time 7 and 60 days respectively, indicating that the severe corrosion of X70 steel occurs in the sandy soil corrosive environment with a smaller particle size. This conclusion was also supported by Bode plots in the phase angle-log (frequency), which give the phase angle of the characterization of the corrosion product film that is the same basically in the initial stage inferring that the integrity of the corrosion product film is essentially the same. Generally, the phase angle is related to the integrity of the corrosion product film [25]. At buried

time increasing up to 60 days, the integrity of corrosion product film of X70 steel decreased with the particle size decreasing. The phase angle characterization of the product film integrity is the same basically when buried 90 days, indicating that the integrity of product film will tend to be equal with the buried time increasing. This may be due to the corrosion products and soil particles glued together forming new particles which are adhered to the metal electrode surface and the structure of the corrosion product film tends to be equal.

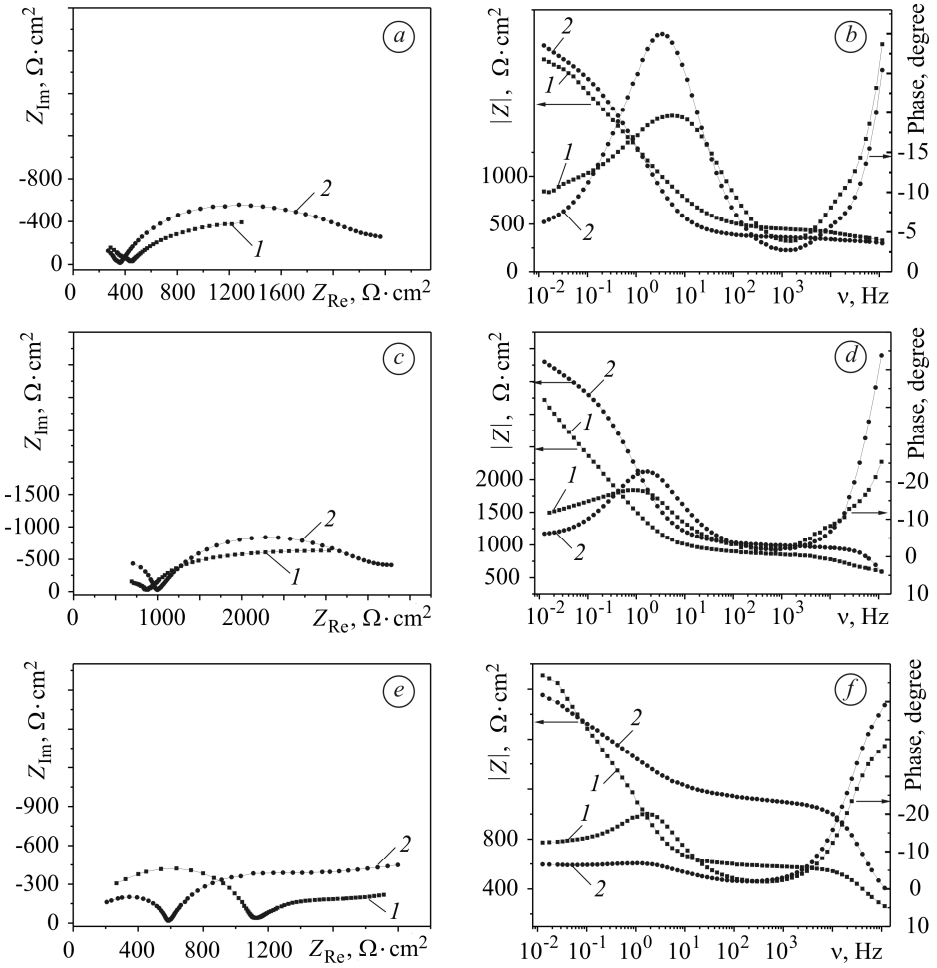

Fig. 4. Nyquist diagrams (*a*, *c*, *e*) and Bode plots (*b*, *d*, *f*) of X70 pipeline steel with buried time of 7 (*a*, *b*), 60 (*c*, *d*) and 90 days (*e*, *f*): *1* – 1# sands; *2* – 2# sands.

The formation of the medium-frequency capacitive loop is mainly due to the charge transfer reaction of X70 steel corrosion process. With the decrease of the particle size, the size of this capacitive loop semicircle decreased, indicating that the charge transfer process was getting more important than the diffusion process with decreasing particle size (corresponding to the proportion of TPB zone per unit area increase), in other words, the cathodic oxygen reduction reaction accelerated with the decrease of the particle size. Furthermore, the magnitude of the frequency impedance is equal to 10 mHz which is inversely proportional to the corrosion rate of metal which decreased with the particle size growth, as shown in Bode plots in the |*Z*|-log (frequency). This result further demonstrates that the corrosion rate of X70 steel in sandy soil solution increases with the particle sizes decreasing.

The presence of low-frequency diffusive impedance, not obvious in Nyquist plots suggests that the mass-transfer of dissolved oxygen plays an essential role in the corrosion process of X70 steel, and the whole corrosion process is mixed-controlled by mass-transfer and diffusion steps. However, the diffusion impedance is linear deviation from the standard of 45° line which may be related to the condition of electrode surface as well as the dispersion effect of electrolyte by soil particles on the metal surface resulting in spherical diffusion.

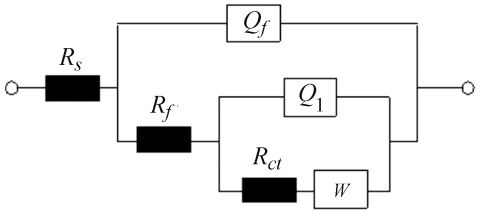

Fig. 5. Equivalent circuit representing the corrosion process of X70 pipeline steel in Fig. 4.

In order to further understand the corrosion mechanisms, the corresponding equivalent circuit for EIS tests of X70 steel fitted by ZSimpWin software was shown in Fig. 5. There are two time constants in the equivalent circuit diagram that can describe the corrosion process of X70 steel in simulated sandy soil solution $R_s(Q_f(R_f(Q_1(R_{ct}W))))$, where R_s is the sandy soil resistance between the working and the reference electrodes, and Q_f–R_f represents the capacitance and resistance of the corrosion product film on the metal surface; R_{ct}–Q_1 corresponds to the charge transfer resistance and a constant phase element (CPE), and W represents the Warburg diffusion impedance which value can be expressed as $Z_w = (Y_w(j\omega)^{0.5})^{-1}$.

The electrochemical parameters which can be obtained by fitting the EIS based on the equivalent circuit in Fig. 5, and are listed in Table 2. It can be seen that, with decreasing sandy soil particle size, the charge transfer resistance (R_{ct}) decreased. In the current study [16], the reciprocal of R_{ct} value was used to characterize the corrosion rate because of its close correlation with the corrosion rate. So, it can be concluded that the corrosion rate of X70 steel increased with decreasing particle size. The EIS data fitting errors of equivalent circuit in Fig. 5 are all within 10% and the effect of fitting is good.

Table 2. EIS fitting results of X70 pipeline steel from the equivalent circuit

Corrosion time	Sands number	R_s, $\Omega\cdot cm^2$	Q_f		R_f, $\Omega\cdot cm^2$	Q_1		R_{ct}, $\Omega\cdot cm^2$	Y_w, $S^{-0.5}\times$ $\times\Omega\cdot cm^{-2}$
			Q_f–Y_f, $S^n\cdot\Omega\cdot cm^{-2}$	Q_f–n_f		Q_1–Y_1, $S^n\cdot\Omega\cdot cm^{-2}$	Q_1–n_1		
7 days	1#	211.2	$7.101\cdot10^{-8}$	0.7796	252.5	$2.159\cdot10^{-4}$	0.6561	1089	$5.626\cdot10^{-3}$
	2#	215.6	$9.852\cdot10^{-8}$	0.9064	361.1	$1.652\cdot10^{-4}$	0.7147	1800	$4.421\cdot10^{-3}$
60 days	1#	236.8	$3.648\cdot10^{-8}$	0.6078	748.7	$3.258\cdot10^{-4}$	0.6360	1948	$4.299\cdot10^{-3}$
	2#	199.6	$9.157\cdot10^{-8}$	0.7161	869.5	$1.436\cdot10^{-4}$	0.7072	2643	$3.628\cdot10^{-3}$
90 days	1#	88.1	$4.944\cdot10^{-8}$	0.8798	1009.3	$6.551\cdot10^{-4}$	0.5035	840	$8.320\cdot10^{-3}$
	2#	90.9	$1.755\cdot10^{-8}$	0.8473	502.4	$2.789\cdot10^{-4}$	0.7473	1089	$6.276\cdot10^{-3}$

However, in the initial stages of the corrosion process up to 60 days, the charge transfer resistance R_{ct} increased with the buried time increasing, which can be attributed to the corrosion products that are formed and adhere to the electrode surface [7]. With increased buried time, the value of R_{ct} decreased resulting from the detachment of lose products. As shown in Nyquist plots (Fig. 4) above, the R_{ct} values also decreased with the particle size decreasing.

The modulus of the Warburg Y_w, reciprocal to the diffusional impedance described in $Z_w = (Y_w(j\omega)^{0.5})^{-1}$, are plotted in Fig. 6. It can be seen that the diffusional impedance increases with decreasing particle size in the same buried time. This can be mainly attributed to the smaller soil particle size with the larger dispersion degree of electrolyte on the metal surface, which leads to the larger proportion of TPB zone per unit area. However, the diffusion process of dissolved oxygen in TPB zone is rapid, leading to the diminished diffusion impedance of the metal in sandy soil corrosive environment with a small particle size. As can be seen in Table 2, with the buried time increase, the diffusional impedance of X70 steel increased slowly. This may be attributed to the electrolyte on the metal surface which is affected by the adherence of new particles that are formed by soil particles and corrosion products, as a consequence, affecting the acceleration of TPB zone on the cathode process. For the lines in Fig. 6, it can be seen obviously that, in the initial stages of the corrosion process up to 60 days, the reciprocal values of Y_w increased over buried time, suggesting that the corrosion rate of X70 steel decreased. Consequently, this result is consistent with the R_{ct} value of X70 steel corrosion process that the charge transfer resistance increased with increasing the buried time in the initial stages of corrosion process.

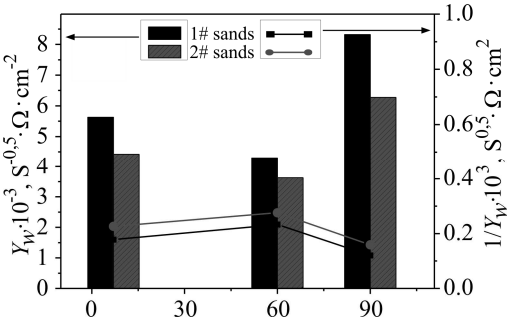

Fig. 6. EIS fitting the Y_w and $1/Y_w$ values of X70 pipeline steel variation buried time. Y_w is the modulus of the Warburg and $1/Y_w$ represents the variation tendency of the diffusional impedance.

The total electrochemical impedance of X70 steel in 3.5 wt.% NaCl sandy soil in Fig. 5 can be represented by the following equation:

$$Z = R_s + \frac{1}{\dfrac{1}{R_f + \dfrac{1}{\dfrac{1}{R_{ct} + Y_w(jw)^{-0.5}} + Y_{Q_1}(jw)^{n_1}}} + Y_{Q_f}(jw)^{n_f}},$$

where R_s, R_f, R_{ct} and Y_w represent soil resistance, the resistance of the corrosion product film, the charge transfer resistance and the modulus of the Warburg, respectively, and ω is the angular frequency (rad/s). Y_{Q_1} is the admittance of constant phase element and Y_{Qf} is the admittance of the corrosion product film. For the equation, the coefficients n_f and n_{dl} represent a depress feature in the Nyquist diagrams. The electrochemical parameters in equation are listed in Table 2.

This relation was derived in the following way. The formula represents the total electrochemical impedance in Fig. 5, and the impedance of the element W is $Y_w(jw)^{-0.5}$, and the total impedance of the elements for R_{ct} and W is added to the R_{ct} and $Y_w(jw)^{-0.5}$ results in R_{ct} and W as a series relationships. However, the element of Q_1 and R_{ct}–W is in parallel connection, and then the total impedance of the elements for Q_1 and R_{ct}–W is added to the Q_1 resistance ($Y_{Q1}(jw)^{n_1}$) and to the reciprocal of the resistance of R_{ct}–W ($\dfrac{1}{R_{ct} + Y_w(jw)^{-0.5}}$). Moreover, the element of R_f and Q_1–R_{ct}–W is

in parallel connection and the impedance for these three elements is added to the R_f and to the reciprocal of the resistance of Q_1–R_{ct}–W ($\frac{1}{\frac{1}{R_{ct}+Y_w(jw)^{-0.5}}+Y_{Q1}(jw)^{n_1}}$). The derivation process of other impedance for the element in Fig. 5 is obtained by the same mode. Hence, the total electrochemical impedance of X70 steel in 3.5 wt.% NaCl sandy soil in Fig. 5 can be represented by the above equation.

According to the results of Table 1 and Table 2, it should be noted that the EIS study results correspond to the polarization results.

Table 3. The (EDS) analysis (wt.%) of products

Elements	1# sands	2# sands
Fe	46.46	52.30
O	31.91	29.44
Si	11.25	10.22
C	7.86	5.43
Cl	2.01	1.86
Na	0.52	0.85

Surface analysis. Fig. 7 gives the corresponding SEM images and EDS of rust layers of X70 steel in 3.5 wt.% NaCl sandy soil after buried for 90 days. It can be seen that, with decreasing particle size, the numbers and sizes of pores in rust layers increased. Moreover, it is worth noting that these pores are mainly composed of two parts, one is the defects of the rust layer itself, and the other is the contact between particle pores. Obviously, the rust layers on X70 steel are generally loose, porous and defective,which resulting in the corrosive ions in soil solution can reach the surface substrate. It can also be seen that the soil particles are wrapped with incomplete film in 1# sands corrosive system, and there are a lot of tiny cracks and pores in the rust layer in 2# sands corrosive system respectively, as shown in Fig. 7*a*, *c*. This also can be attributed to the morphologies of SiO_2, a composition of soil particles on the surface of metal [25]. The morphology of metal surface corrosion of X70 steel after removing corrosion products is further analyzed below.

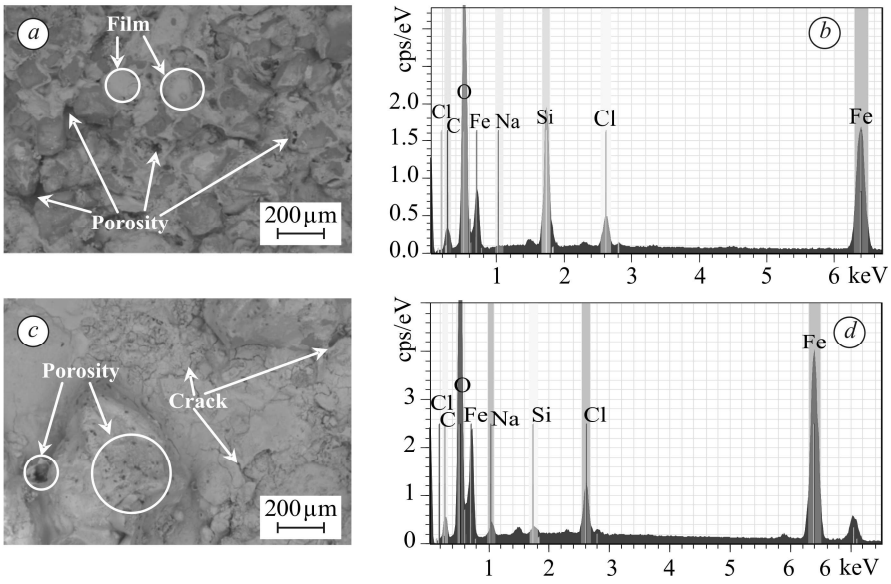

Fig. 7. The SEM images (*a* – 1# sands system; *c* – 2# sands system) and EDS spectrum (*b* – 1# sands system; *d* – 2# sands system) of rust layer formed on X70 steel surface after 90 days buried.

The EDS analysis results of the product film are shown in Fig. 7*b*, *d*. The main elements of corrosion products of X70 steel in NaCl sandy soil are listed in Table 3. The elements of Na and Cl are mainly from NaCl contaminated soils, and Si may come from the standard quartz sand and the substrate itself.

In order to further understand the composition of corrosion products, the products were observed by X-ray diffraction analysis (XRD), as shown in Fig. 8. Clearly, the compositions of products consist of SiO_2, FeOOH, Fe_3O_4 and Fe_2O_3. In addition, SiO_2 is the main ingredient of soil particles such as quartz sand.

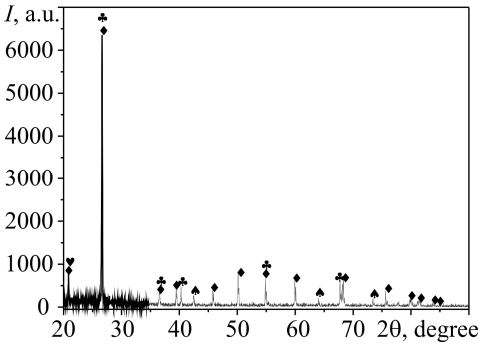

Fig. 8. X-ray diffraction characterization of corrosion products: ♦– SiO_2; ♣ – FeOOH; ♥ – Fe_3O_4; ♠ – Fe_2O_3.

The surface morphology of the buried specimens of X70 steel after removing rust layers were observed by SEM, as shown in Fig. 9. It is apparent that the surface of X70 steel was strongly damaged in the soil corrosive environment with the particle size equal to 0.1…0.25 mm. The roughness of the corroded surfaces increases with the particle size decreasing. This is attributed to the inhomogeneity of the rust layer formed. As can be seen in Fig. 9, with particle size decreasing, the number and size of pits increased obviously, inferring that the corrosion rate of X70 steel reduced with the sandy soil particle size increasing. As a consequence, the surface analysis results agree well with the results of the electrochemical studies.

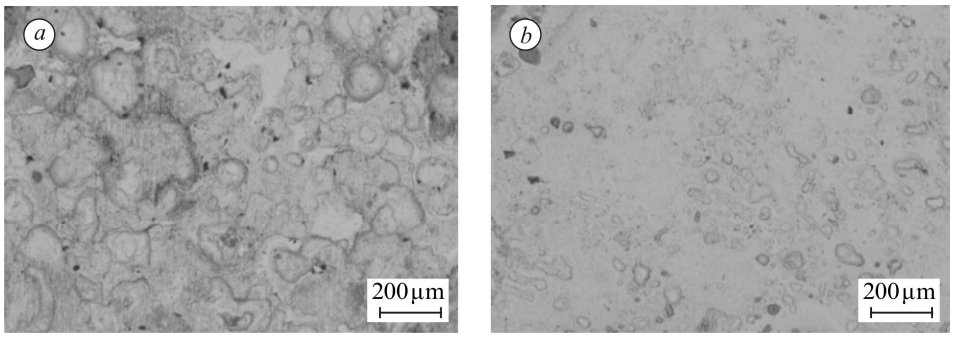

Fig. 9. Surface images of X70 pipeline steel after removing corrosion products: *a* – 1# sands; *b* – 2# sands.

CONCLUSIONS

The polarization resistance of X70 steel decreases with decreasing particle size in 3.5 wt.% NaCl simulated sandy soil corrosive environment, and the corrosion rate of X70 steel increases with decreasing particle size. The corrosion tendency of sandy soil increases with buried time. The anode branch slopes of polarization curve of X70 steel corrosion process are basically the same, but, the right shift of the cathodic branch with a particle size of sandy soil decreasing, suggests that the cathode oxygen reduction process is accelerated, and the proportion of gas/liquid/solid (TPB) zone also increased with the particle size decreasing. Thus, the acceleration of cathode corrosion process is more significant. The corrosion of X70 steel is controlled by the process of cathode diffusion and oxygen reduction. There are two time constants in the equivalent circuit diagram that can describe the corrosion process of X70 steel in 3.5 wt.% NaCl sandy

soil corrosive environment, as description of $R_s(Q_f(R_f(Q_1(R_{ct}W))))$. Furthermore, the diffusional impedance of X70 steel decreases with decreasing particle size. The corrosion rust layers of X70 steel after buried 90 days are generally loose, porous, incomplete and defective, and provide minor protection of the matrix; the corrosion products adhere with soil particles forming new particles, which also influence the proportion of TPB zone per unit area on the metal surface. Furthermore, the number and sizes of corrosion pits (spots) increase with the particle size decrease. The results of this work can provide necessary references and theoretical basis for actual anti-corrosion researches of the natural gas pipelines. It suggests that, in choosing the backfill soil for the construction process of buried pipelines, the advantage choice should be given to relatively large sandy particle-size as backfill materials.

РЕЗЮМЕ. З допомогою методів потенціодинамічних поляризаційних кривих та електрохімічної імпедансної спектроскопії (EIS) досліджено корозійну поведінку трубопровідної сталі X70 у ґрунтовому середовищі, яке змодельовано розчином 3,5 wt.% NaCl з частинками кварцового піску різного розміру (0,1…0,25 і 0,6…1,0 mm). Встановлено, що швидкість корозії сталі зростає зі зменшенням розміру частинок ґрунту, про що свідчить зниження її поляризаційного опору, а також зсув катодних гілок поляризаційних кривих вправо. Зроблено висновок, що в цьому випадку корозію сталі контролює катодний процес відновлення кисню на межі поділу метал–середовище, інтенсивність якого зростає зі зменшенням розміру частинок ґрунту.

РЕЗЮМЕ. С помощью методов потенциодинамических поляризационных кривых и электрохимической импедансной спектроскопии (EIS) исследовано коррозионное поведение трубопроводной стали X70 в почвенной среде, которую моделировали раствором 3,5 wt.% NaCl с частицами кварцевого песка разного размера (0,1…0,25 и 0,6...1,0 mm). Установлено, что скорость коррозии стали растет с уменьшением размера частиц почвы, о чем свидетельствует снижение ее поляризационного сопротивления, а также сдвиг катодных ветвей поляризационных кривых вправо. Сделан вывод, что в данном случае коррозию стали контролирует катодный процесс возобновления кислорода на грани деления металл–среда, нитенсивность которого растет с уменьшением размера частиц почвы.

1. *Cole I. S. and Marney D.* Modelling steel corrosion damage in soil environment // Corros. Sci. – 2012. – **56**. – P. 5–16.
2. *Piao S. L., Fang J. Y., and Liu H. Y.* NDVI-indicated decline in desertification in China in the past two decades // Geophys. Res. Lett. – 2005. – **32**, № 6. – P. 1–4.
3. *Syrotyuk A. M. and Dmytrakh I. M.* Methods for the evaluation of fracture and strength of pipeline steels and structures under the action of working media. Part I. Influence of the corrosion factor // Materials Science. – 2014. – **50**, № 3. – P. 324–339.
4. *Jeannin M., Calonnec D., and Sabot R.* Stress corrosion cracking behavior of X70 pipe steel in an acidic soil environment // Corros. Sci. – 2010. – **52**. – P. 2026–2034.
5. *Fu J., Pei F., and Zhu Z. P.* Influence of moisture on corrosion behavior of steel ground rods in mildly desertified soil // Anti-Corros. Methods Mater. – 2013. – **60**, № 3. – P. 148–152.
6. *Kakooei S., Hossein T., and Ismail M. C.* Corrosion investigation of pipeline steel in hydrogen sulfide containing solutions // J. Appl. Sci. – 2012. – **12**, № 23. – P. 2454–2458.
7. *Lopes I. M. F., Louriro C. R. O., and Junqueira R. M. R.* Corrosion monitoring of galvanized steel in soil extract solutions by electrochemical impedance spectroscopy // Materialwiss. Werkstofftech. – 2014. – **45**, № 7. – P. 619–627.
8. *Wang J.* Electrochemical study on corrosion behaviour of steels in sand with water // Chin. J. Oceanol. Limnol. – 1997. – **15**, № 4. – P. 369–372.
9. *Jiang J. and Wang J.* The role of cathodic distribution in gas/liquid/solid multiphase corrosion systems // J. Solid State Electrochem. – 2009. – **13**. – P. 1723–1728.
10. *Jiang J., Wang J., and Lu Y. H.* Effect of length of gas/liquid/solid three-phase boundary zone on cathodic and corrosion behavior of metals // Electrochim. Acta. – 2009. – **54**. – P. 1426–1435.

11. *Jiang J., Wang J., and Wang W. W.* Modeling influence of gas/liquid/solid three-phase boundary zone on cathodic process of soil corrosion // Electrochim. Acta. – 2009. – **54**. – P. 3623–2629.
12. *Wang J. and Jiang J.* The role of electrochemical polarization in micro-droplets formation // Electrochem. Commun. – 2008. – **10**, № 11. – P. 1788–1791.
13. *Wang Y. H., Liu Y. Y., and Wang W.* Influences of the three-phase boundary on the electrochemical corrosion characteristics of carbon steel under droplets // Mater. Corros. – 2013. – **64**, № 4. – P. 309–313.
14. *Murray J. N. and Moran F. J.* Influence of moisture on corrosion of pipeline steel in soils using in situ impedance spectroscopy // Corrosion. – 1989. – **45**, № 1. – P. 34–43.
15. *Glazov N. N., Ukhlovtsev S. M., and Reformatskaya I. I.* Corrosion of carbon steel in soils of varying moisture content // Protec. Met. – 2006. – **42**. – P. 601–608.
16. *Lorenz W. J. and Mansfeid F.* Determination of corrosion rates by electrochemical DC and AC methods // Corros. Sci. – 1981. – **21**, № 9–10. – P. 647–672.
17. *Pernic P., Arpaia M., and Cistantini A.* Application of the generalized Jaroniec–Choma isotherm equation for describing benzene adsorption on acttvated carbons // Mater. Chem. Phys. – 1990. – **25**, № 3. – P. 323–330.
18. *Zhang L., Li X. G., and Du C. W.* Effect of environmental factors on electrochemical behavior of X70 pipeline steel in simulated soil solution // J. Iron Steel Res. Int. – 2009. – **16**, № 6. – P. 52–57.
19. *McCafferty E.* Validation of corrosion rates measured by the Tafel extrapolation method // Corros. Sci. – 2005. – **47**. – P. 3202–3215.
20. *Choi Y. S. and Kim J. G.* Aqueous corrosion behavior of weathering steel and carbon steel in acid-chloride environments // Corrosion. – 2000. – **56**, № 12. – P. 1202–1210.
21. *Influence* of ultrasound power and frequency upon corrosion kinetics of zinc in saline media / M. L. Doche, J. Y. Hihn, A. Mandroyan, R. Viennet, and F. Touyeras // Ultrason. Sonochem. – 2003. – **10**. – P. 357–362.
22. *Study* of cavitation corrosion behaviors and mechanism of carbon steel in neutral sodium chloride aqueous solution / J. Liu, Y. Lin, X. Yong, and X. Li // Corrosion. – 2005. – **61**. – P. 1061–1069.
23. *Cao C. N. and Zhang J. Q.* Introduction to the electrochemical impedance spectra. – Beijing: Science Press., 2002. – P. 98–103.
24. *Ozcan M.* Organic sulphur-containing compounds as corrosion inhibitors for mild steel in acidic media: correlation between inhibition efficiency and chemical structure // Appl. Surf. Sci. – 2004. – **236**, № 1–4. – P. 155–164.
25. *Gu K. M., Lv L. Y., and Lu Z. L.* Electrochemical corrosion and impedance study of SAE1045 steel under gel-like environment // Corros. Sci. – 2013. – **74**. – P. 408–413.

Received 30.03.2015